Title

Model training periods impact estimation of COVID-19 incidence from wastewater viral loads.

Journal

The Science of the total environment, 858(Pt 1)

ISSN

0048-9697

Authors

Daza-Torres, Maria L
Montesinos-López, J Cricelio
Kim, Minji
et al.

Publication Date

2023-02-01

DOI

10.1016/j.scitotenv.2022.159680

Since January 2020 Elsevier has created a COVID-19 resource centre with free information in English and Mandarin on the novel coronavirus COVID-19. The COVID-19 resource centre is hosted on Elsevier Connect, the company's public news and information website.

Science of the Total Environment 858 (2023) 159680

Contents lists available at ScienceDirect

Science of the Total Environment

journal homepage: www.elsevier.com/locate/scitotenv

Model training periods impact estimation of COVID-19 incidence from wastewater viral loads

Maria L. Daza-Torres [a,*,1], J. Cricelio Montesinos-López [a,1], Minji Kim [b], Rachel Olson [c], C. Winston Bess [c], Lezlie Rueda [b], Mirjana Susa [a], Linnea Tucker [c], Yury E. García [a], Alec J. Schmidt [a], Colleen C. Naughton [d], Brad H. Pollock [a], Karen Shapiro [b], Miriam Nuño [a], Heather N. Bischel [c,*]

[a] Department of Public Health Sciences, University of California Davis, Davis, CA 95616, United States
[b] Department of Pathology, Microbiology and Immunology, School of Veterinary Medicine, University of California Davis, Davis, CA 95616, United States
[c] Department of Civil and Environmental Engineering, University of California Davis, Davis, CA 95616, United States
[d] Department of Civil and Environmental Engineering, University of California Merced, Merced, CA 95343, United States

HIGHLIGHTS

- We introduce two models to relate SARS-CoV-2 wastewater data to clinical case data.
- Adequate training periods are essential for accurate projection of cases.
- A testing period is classified as adequate when test rates exceed case rates.
- Similar case projections were obtained using the two models.
- The effective reproductive number was estimated using case predictions.

GRAPHICAL ABSTRACT

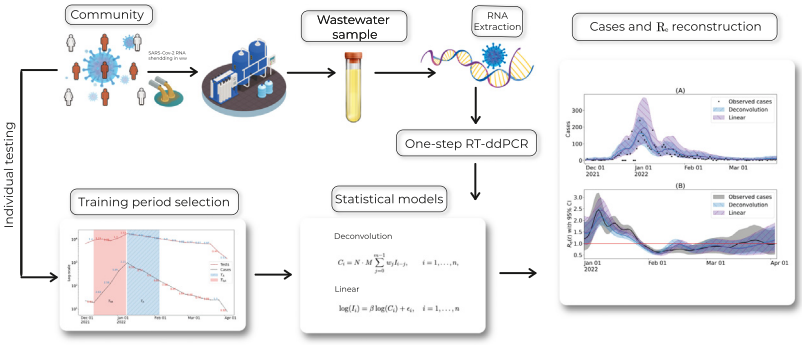

ARTICLE INFO

Editor: Damia Barcelo

Keywords:
SARS-CoV-2
COVID–19
Wastewater-based epidemiology (WBE)
Public health surveillance: sewage
Bayesian inference
Statistical models

ABSTRACT

Wastewater-based epidemiology (WBE) has been deployed broadly as an early warning tool for emerging COVID-19 outbreaks. WBE can inform targeted interventions and identify communities with high transmission, enabling quick and effective responses. As the wastewater (WW) becomes an increasingly important indicator for COVID-19 transmission, more robust methods and metrics are needed to guide public health decision-making. This research aimed to develop and implement a mathematical framework to infer incident cases of COVID-19 from SARS-CoV-2 levels measured in WW. We propose a classification scheme to assess the adequacy of model training periods based on clinical testing rates and assess the sensitivity of model predictions to training periods. A testing period is classified as adequate when the rate of change in testing is greater than the rate of change in cases. We present a Bayesian deconvolution and linear regression model to estimate COVID-19 cases from WW data. The effective reproductive number is estimated from reconstructed cases using WW. The proposed modeling framework was applied to three Northern California communities served by distinct WW treatment plants. The results showed that training periods with adequate testing are essential to provide accurate projections of COVID-19 incidence.

1. Introduction

During the early phases of the COVID-19 pandemic, caused by the severe acute respiratory syndrome coronavirus 2 (SARS-CoV-2), the World Health

* Corresponding authors.
E-mail addresses: mdazatorres@ucdavis.edu (M.L. Daza-Torres), hbischel@ucdavis.edu (H.N. Bischel).
[1] Co-first author.

http://dx.doi.org/10.1016/j.scitotenv.2022.159680
Received 1 August 2022; Received in revised form 19 October 2022; Accepted 20 October 2022
Available online 26 October 2022

Organization (WHO) recommended implementing mass testing programs as a containment measure. Individual diagnostic testing informs contact tracing and medical interventions, ideally cutting chains of transmission short and containing outbreaks. Mass clinical screening programs can also provide valuable data on community-level health trends, but maintaining mass testing programs for the purpose of community-level monitoring is expensive and requires robust infrastructure with consistent availability of testing supplies and human resources (Vandenberg et al., 2021). Moreover, diagnostic tests validated in low-throughput clinical settings (like nucleic acid amplification tests or NAATs) are not necessarily efficient platforms for constructing community screening programs (Raffle et al., 2020). Design-wise, employing such tests for large-scale screening requires extensive logistical coordination over large geographic areas. This becomes especially complicated when the options for diagnostic tests are myriad, lack standardization, and depend heavily on local social landscapes. Small biases in the tests may be inflated when deployed broadly, leading to large spurious associations at the population level (Mardian et al., 2021; Mercer and Salit, 2021).

Public health authorities are turning to wastewater-based epidemiology (WBE) as an alternative strategy for less-biased population-level surveillance of COVID-19. WBE uses biomarkers in wastewater (WW) to monitor trends in community-level health indices. WBE methods have been used to detect changes in drug consumption (Castiglioni et al., 2014; Zuccato et al., 2005), dietary patterns (Choi et al., 2019), and the circulation of pathogens like poliovirus and norovirus (Asghar et al., 2014). Measurements of SARS-CoV-2 RNA in WW correlate strongly with changes in COVID-19 prevalence in the associated communities (Huisman et al., 2022; McMahan et al., 2021; Vallejo et al., 2022; Wolfe et al., 2021). Since the onset of the pandemic, WBE of SARS-CoV-2 has been implemented in over 67 countries and 279 universities (COVIDPoops19, 2021). In some places, WBE programs have detected changes in SARS-CoV-2 RNA levels in WW prior to changes in local COVID-19 hospitalization activity and spikes in NAAT screening cases (Kirby et al., 2022; Mallapaty et al., 2020; Medema et al., 2020b; Peccia et al., 2020; Shah et al., 2022; Wurtzer et al., 2020). Others have used WBE to assess the effectiveness of public health interventions (Pillay et al., 2021), and recently, WBE was used to predict hospitalizations and ICU admissions (Galani et al., 2022). In addition to monitoring trends, WBE can provide estimates of critical disease transmission parameters in the community without the biases associated with test-seeking behavior or poor access to testing programs.

An ongoing challenge for WBE is developing robust data collection and interpretation methods that are comparable across time and geography. Variations in sampling design and sample processing methods, natural variability in viral shedding rates in feces, variability in WW flow volume, population fluctuations, and location-specific characteristics of WW management are all factors that make inference of new COVID-19 cases from WW data challenging (Ahmed et al., 2020; Hill et al., 2020; Medema et al., 2020a; Zhu et al., 2021). Such factors will ultimately affect uncertainty estimates when modeling disease incidence and other public health indicators. An ideal WBE program would implement a generalized approach that provides consistent estimates of disease burden in a targeted population, yielding public health metrics like the disease incidence, disease prevalence and/or the effective reproductive number (R_e). Previous studies that approach this problem include: simple algebraic adjustments with environmental constants (Monteiro et al., 2022); estimating the total number of cases with a susceptible-exposed-infectious-recovered (SEIR) model informed by WW results (McMahan et al., 2021); using regression analysis to estimate the number of infected people (Vallejo et al., 2022); and making near real-time estimates of R_e (Huisman et al., 2022; Schoen et al., 2022).

We propose and compare two modeling approaches: a simple linear model and a Bayesian deconvolution approach to estimate COVID-19 incident cases from WW viral loads. Both models rely on short training periods to calibrate WW measurements using clinical testing data from a community screening program. We evaluate the impact of different training periods on model predictions, hypothesizing that relative rates of change in clinical testing and reported cases can be used to identify appropriate model training periods. We then apply the framework to estimate incident cases and R_e from WW influent data generated for three communities in Northern California. The methodology we describe can be generalized to other WBE systems to track the evolution and assess the magnitude of COVID-19 fluctuations and outbreaks in a manner that is comparable across programs, locations, and time.

2. Material and methods

The analytical framework was developed using data from the City of Davis (Davis) and replicated for the City of Woodland and the University of California Davis (UC Davis). The analysis includes case and WW data from December 1, 2021, to March 31, 2022. Results for the City of Woodland and UC Davis are presented in Appendices C and D, respectively.

2.1. Wastewater sample collection

Staff from three Northern California WW treatment facilities (Davis, Woodland, and UC Davis) provided 24-hour composite WW samples 5–7 days per week. Samples were acquired using Teledyne ISCO 5800 refrigerated autosamplers in Davis and Woodland and a Hach Sigma 900 autosampler for UC Davis. The autosampler in Davis was programmed to collect 400 mL of influent every 15 "pulses", where one pulse was set at 10,000 gal. An average of 24 pulses was expected per day based on an average daily influent flow of 3.6 million gallons per day (MGD). The autosampler in Woodland was programmed to acquire 100 mL of influent every 15 min over a 24-hour period. The autosampler for UC Davis was programmed to acquire approximately 200 mL of influent every 20 min over a 24-hour period. The reported sample collection date corresponded to the date when an autosampler program was completed. Davis and UC Davis provided 12 mL samples in new 15-mL polypropylene centrifuge tubes. Woodland provided 1 L samples in Nalgene bottles that were washed, sterilized, and reused over the duration of sampling. Samples were stored at 4 °C and transported weekly in coolers on ice to the analytical lab at UC Davis. For biosafety compliance, samples were placed in a water bath set at 60 °C for 30 min and returned to 4 °C prior to sample processing. Concentration and extraction were performed in a biosafety level 2 (BSL2)-certified laboratory.

2.2. Sample concentration and extraction

The sample concentration and extraction protocol were adapted from Karthikeyan et al. (2021) using 4.875 mL instead of 10 mL starting sample volume. Each WW sample was deposited into a separate well of a KingFisher 24 deep-well plate (Thermo Fisher). An extraction control blank (nuclease-free water) was included in 90 % of the deep-well plates to assess potential contamination during concentration and extraction. Each well was spiked with 50 μL of Nanotrap® Enhancement Reagent 1 (Ceres Nanosciences product ER1 SKU # 10111-10, 10111-30) and 5 μL of a stock of vaccine-strain Bovine Coronavirus (BCoV, Bovilis® Coronavirus vaccine) containing an estimated 1.3×10^8 gc/mL as measured by ddPCR. 500 μL aliquots of the initial BCoV vaccine stock, prepared from the suspension of lyophilized BCoV vaccine in 20 mL buffer provided with the kit, were stored at −80 °C prior to use. Each spiked sample was manually agitated by pipetting up and down at least three times using a 5 mL pipette. Samples were then incubated for 30 min at room temperature. Following incubation, concentration was carried out using 75 μL Nanotrap® Magnetic Virus Particles (Ceres Nanosciences) on a KingFisher Apex robot (Thermo Scientific). Concentrated viruses were eluted from the Nanotrap® beads into 400 mL of lysis buffer per sample from the MagMAX Microbiome Ultra Nucleic Acid Isolation Kit (Thermo Fisher). Concentrated samples were extracted per the MagMAX kit manufacturer instructions in 96 deep-well plates on the KingFisher Apex. Samples were eluted in 100 μL of MagMAX Elution Solution. Extracts were typically stored on ice and immediately subjected to same-day analysis. When the same-day analysis was not possible, extracts were immediately stored at −80 °C until analysis.

2.3. Extract analysis by ddPCR

Sample extracts were analyzed by digital droplet polymerase chain reaction (ddPCR) for four targets: N1 and N2 targeting regions of the nucleocapsid (N) gene of SARS-CoV-2, and Bovine Coronavirus (BCoV) and pepper mild mottle virus (PMMoV) for normalization of the SARS-CoV-2 results. N1/N2 and BCoV/PMMoV were quantified in separate duplex assays. Due to high levels of PMMoV, the sample for the PMMoV/BCoV duplex was diluted 40× prior to loading. The duplex ddPCR amplifications were performed in 20 μL reactions on a QX ONE ddPCR System (Bio-Rad). Each reaction contained the following components: 1× Supermix, 20 U/μL Reverse transcriptase, 15 mM Dithiothreitol from the One-Step RT-ddPCR Advanced Kit for Probe (Bio-Rad), 900 nM of each primer, 250 nM of each probe, and 5 μL of sample extract or control. The one-step ddPCR reaction consisted of 3 min plate equilibrium at 25 ° C, 60 min reverse transcription at 50 ° C, 10 min enzyme activation at 95 ° C, followed by 40 cycles of 30 s denaturation at 94 ° C and 1 min annealing/extension at 58 ° C, and then 10 min enzyme deactivation at 98 ° C and 1 min droplet stabilization at 25 ° C. Preparation and plating of ddPCR master mix were carried out in a separate location from sample loading to avoid contamination. Sample loading was performed using an epMotionR 5075 (Eppendorf) liquid handler. Each ddPCR plate included duplicate positive controls (stock mixture of synthesized gene fragments containing for the four target regions) for each target and duplicated no-template controls (nuclease free water). Additional information on the ddPCR assay designs is available in Appendix A. Table A.1 summarizes primers, probes for ddPCR assays performed as part of this work. Tables A.2 and A.3 provide the ddPCR reaction and 20× primer/probe mix recipes. From October 21 to December 21, Cy5 and Cy5.5 were used in place of FAM and HEX as the fluorophores for PMMoV and BCoV, respectively. Table A.4 lists details for the positive controls. Prior to 12/21/22 the annealing temperature was 60 ° C. The selection of positive and negative droplet clusters in samples and controls was conducted manually based on visual inspection of clusters. Results were considered invalid if the distribution of positive or negative droplets appeared abnormal in shape or if the total number of droplets generated fell below a threshold of 10,000 droplets in a single well.

2.4. Laboratory quality control and data processing

The sensitivity of the analytical assay was assessed by determining a limit of detection (LOD) and a limit of blank (LOB) following protocols recommended by the ddPCR manufacturer (Bio-Rad Laboratories, 2021, A practical guide for evaluating detection capability using ddPCR). Fifteen WW samples that were initially screened as negative for SARS-CoV-2 in routine WW ddPCR monitoring (i.e., extracts had less than 4 positive droplets in merged wells from duplicate analysis) were used to determine the lowest detectable concentrations in ostensibly blank WW samples. Selection of these extracts provided a conservative approach to determining the LOB. The selected extracts were re-analyzed by ddPCR to obtain data for four additional replicates for each sample. A non-parametric (rank order) method was then used to select the LOB, since results from the blank were not normally distributed. The ddPCR number of droplets from individual wells was tabulated from lowest to highest. The LOB was set at the value of the concentration measurement for the rank position corresponding to the 95th percentile, calculated as follows: $Rank = 0.5 + 0.95^{*}$ (number of measurements). Since the calculated rank position was a non-integer value, the rank position was rounded up to provide a more conservative LOB. The theoretical LOD was set as the LOB plus two times the standard deviation of all replicate results (Biorad, 2021). The LOD and LOB are reported in Table A.5. In terms of droplet numbers in the blank samples, the highest numbers of positive droplets in the merged wells (four replicates) amongst the fifteen blank samples were 6 (N1) and 8 (N2). Since routine WW samples were analyzed in duplicate, 3 (N1) and 4 (N2) droplets were set as the cutoff to mark samples below the droplet threshold. Samples were also considered below the droplet threshold if there were fewer N1 and N2 droplets than twice the number of droplets in the extraction control blank analyzed on the same day. Runs with an extraction control blank that had >15 positive droplets in either N1 or N2 were considered contaminated and extracts were re-processed.

If samples passed all checks, the relative concentration of N gene was calculated as follows. Duplicate results for each target were merged, and the concentration of each target in the ddPCR reaction was calculated assuming a Poisson distribution using the QXOne Software 1.1.1 Standard Addition (Bio-Rad). The average SARS-CoV-2 RNA concentration in the initial WW sample was calculated from the average of the N1 and N2 results, corrected for sample and reagent volumes used, and reported as genome copies (gc) per mL WW. BCoV was detected in 100 % of spiked samples, and concentrations of targets were not corrected for BCoV recovery efficiency. If N1 or N2 merged droplet counts were below the minimum droplet threshold, the target was excluded from the average concentration. If both N1 and N2 targets were below the droplet threshold, the concentration was reported as 0. We utilize N/PMMoV (the average SARS-CoV-2 RNA concentration (N) divided by the concentration of PMMoV) as the resulting WW signal for subsequent model development.

2.5. COVID-19 case data

Healthy Davis Together (HDT) and Healthy Yolo Together (HYT) provided daily COVID-19 cases and total tests performed during the study period for Davis, UC Davis, and Woodland, from the community screening program (HDT, 2020; HYT, 2021). HDT was a program implemented in the city of Davis as an effort to mitigate the spread of COVID-19 and facilitate the return “normal”. The citywide effort launched in September 2020 before expanding to the rest of Yolo County the following July as part of a re-branded HYT. The program involved free saliva-based asymptomatic and symptomatic testing with high throughput methods to process large volumes of tests.

Daily observations of cases were smoothed for implementing the linear model using a 7-day moving average (the mean of the current and the previous six days). This approach improves harmonization between the current WW concentration and observed cases (Fig. 1B). The 7-day moving average of cases for the linear model is similar to a deconvolution model

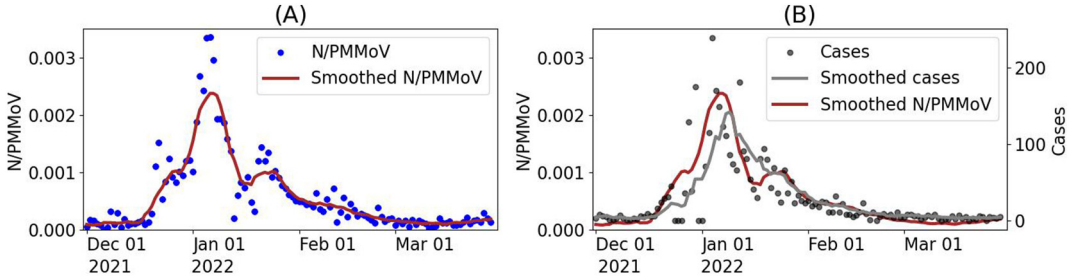

Fig. 1. (A) Raw wastewater data (N/PMMoV) and 10-day moving average of WW data (Smoothed N/PMMoV). (B) Raw cases (Cases), 7-day moving average of cases (Smoothed cases), and 10-day moving average of WW data.

with equal weights (uniform shedding load distribution) and a shedding time of 7 days (Section 2.7.1). The rate of change for tests administered and positive cases were calculated from a weekly aggregation of daily test counts and positive cases identified. Changes in test and case rates were then used to determine training periods with adequate testing.

2.6. Smoothed wastewater signal

To reduce uncertainty and minimize daily fluctuations of WW data, we applied a 10-day moving average for daily influent WW data (Fig. 1A). We use the resulting smoothed influent WW data to correlate with raw cases in the deconvolution model and smoothed cases in the linear model (Fig. 1B).

2.7. Models

We present two models to estimate COVID-19 cases from SARS-CoV-2 RNA in the WW. The first model was adapted from Huisman et al.'s (2022) approach and relates past infections with WW signal through the convolution described in Eq. (3). The number of daily cases is modeled with a Negative Binomial (NB) distribution through the deconvolution (the inverse operation of convolution) noted in Eq. (3). The second approach uses a simple linear regression to estimate 7-day moving average of cases (dependent variable) from WW data (independent variable). We also propose a strategy for selecting model training periods with adequate clinical testing to estimate parameters and improve estimation.

2.7.1. Deconvolution model

Viral RNA concentrations measured in WW (C_i's) are related to the number of new infections per day (I_i's) through the profile of SARS-CoV-2 RNA shedding in the WW by an infected individual days after infection or symptom onset (Huisman et al., 2022). The measurement C_i of WW on day i is related to infections I_j on prior day j through the following convolution:

$$C_i = N \cdot M \sum_{j=0}^{m-1} w_j I_{i-j}, \qquad i = 1, \ldots, n, \tag{1}$$

where $w_j, j = 1, \ldots, m$ (sums to 1) is the shedding load distribution describing the temporal dynamics of shedding and m is the duration of viral shedding or shedding time. The normalization factor N represents the total virus shed by an infected individual during the infection period. M is a constant that depends on the sewer system, WW treatment plant, and processing pipeline.

The measurement of viral RNA in WW, C_i on the day i, is used to estimate COVID-19 cases from WW concentration data via convolution. As noted by Huisman et al. (2022), normalization factors N and M are difficult to measure, and they assume $B = N \cdot M$ as the lowest concentration of the viral load or concentration from a single infection (Huisman et al., 2022). The weights for shedding load distribution (w_j) can be estimated using individual-pooled analysis of SARS-CoV-2 viral loads (Cevik et al., 2020; Weiss et al., 2020; Xu et al., 2020). Instead, we estimate B and corresponding weights using measured WW data and cases within a specified period (training period) by directly modeling the deconvolution process through a Bayesian approach.

We model w_j as follows:

$$w_j = \frac{f_b(j)}{\sum_{k=0}^{m-1} f_b(k)}, \qquad j = 0, 1, \ldots, m-1,$$

where $f_b(k)$ is the probability density function (PDF) of a random variable X with exponential distribution of rate parameter b. Hereafter, notation w_j^b will be used instead of w_j emphasizing that weights depends on parameter b. Note that, if $X \sim Exp(b)$ then its PDF is $f_b(k) = be^{-b \cdot k}$, thus:

$$w_j^b = \frac{be^{-b \cdot k}}{\sum_{k=0}^{m-1} be^{-b \cdot k}} = \frac{e^{-b \cdot k}}{\sum_{k=0}^{m-1} e^{-b \cdot k}}, \qquad j = 0, 1, \ldots, m-1. \tag{2}$$

Eq. (1) is rewritten using Eq. (2) as follows:

$$C_i = B \sum_{j=0}^{m-1} w_j^b \times I_{i-j}. \tag{3}$$

The deconvolution of the Eq. (3) will be denoted as $dec(\mathbf{C}, B, b)$, where $\mathbf{C} = (C_1, C_2, \ldots, C_n)$ represents the vector of WW data, and parameters B and b are described above. $\mathbf{I} = (I_1, I_2, \ldots, I_n)$ correspond to daily cases counts. The theoretical expectation of $\mathbf{I}$ is given by $\mathbb{E}(\mathbf{I}) = \mu$ and it is estimated in terms of the deconvolution model as $\mu = (\mu_1, \mu_2, \ldots, \mu_n) = dec(\mathbf{C}, B, b)$. The deconvolution is approximated using the Richardson–Lucy algorithm (Goldstein et al., 2009).

2.7.1.1. Observational model. We estimate the number of COVID-19 cases per day (I_i) using the NB regression, which is most relevant for overdispersed count data. In this situation, the variance exceeds the mean. The NB distribution describes a sequence of independent and identically distributed Bernoulli trials with a probability of success p before a specified (non-random) number of successes (r) occurs. Assuming a similar approach as in Lindén and Mäntyniemi (2011), we reparametrized the NB distribution in terms of its mean μ and "overdispersion" parameters ω and α, with $r = \frac{\mu}{\omega - 1 + \alpha\mu}$ and $p = \frac{1}{w + \alpha\mu}$ in the usual NB parametrization. We assume that I_i follows a NB distribution. Denoting the mean and variance as μ_i and σ_i^2, respectively, and requiring that $\sigma_i^2 = \omega\mu_i + \alpha\mu_i^2 > \mu_i$, we enforce overdispersion for suitable chosen parameters ω and α. The index of dispersion is $\frac{\sigma_i^2}{\mu_i} = \omega + \alpha\mu_i$. Overdispersion concerning the Poisson distribution is achieved when $\omega > 1$ and the index of dispersion increases with size if $\alpha \neq 0$, adding variability as counts increase. We found good performance fixing $\omega = 2$ and $\alpha = 0.05$, implying higher variability for the later.

Using the deconvolution model and parameter as described above, we obtain the following likelihood function with the assumed NB model:

$$L(\theta|\mathbf{C}, \mathbf{I}) = \prod_{i=1}^{n} \binom{I_i + r_i - 1}{r_i - 1} p_i^{r_i} (1 - p_i)^{I_i},$$

where $r_i = \frac{\mu_i}{\omega - 1 + \alpha\mu_i}$ is the number of successes, $p_i = \frac{1}{\omega + \alpha\mu_i}$ is the probability of a single success, and $(\mu_1, \mu_2, \ldots, \mu_n) = dec(\mathbf{C}, B, b)$.

We estimate $\theta = (B, b)$ from measurements of WW data $\mathbf{C} = (C_1, C_2, \ldots, C_n)$ and daily observations of COVID-19 cases $\mathbf{I} = (I_1, I_2, \ldots, I_n)$. We adopt a Bayesian statistical approach, which is well suited to model multiple sources of uncertainty and allows the incorporation of background knowledge on the model's parameters. In this framework, a prior distribution, $\pi_\Theta(\theta)$, is required to account for unknown parameter θ in order to obtain the posterior distribution. For b, we assumed a Gamma distribution with shape and scale parameters $\nu_b = 2$ and $S_b = 1$, respectively; this assumption is based on published data on viral shedding duration in gastrointestinal samples (Benefield et al., 2020). For B, we assumed a Gamma distribution with shape and scale parameters $\nu_M = 2$ and $S_M = 2/1e^{-4}$, respectively; based on the lowest viral RNA concentrations observed (Huisman et al., 2022). Having specified the likelihood and the prior, we use Bayes' rule to calculate the posterior distribution,

$$\pi_{\Theta|\mathbf{C},\mathbf{I}}(\theta|\mathbf{C}, \mathbf{I}) = \frac{\pi_\Theta(\theta) L(\theta|\mathbf{C}, \mathbf{I})}{Z(\mathbf{I})},$$

where $Z(\mathbf{I}) = \int \pi_\Theta(\theta) L(\theta|\mathbf{C}, \mathbf{I}) d\theta$ is the normalization constant. The posterior distribution is simulated using an existing Markov chain Monte Carlo (MCMC) method, the t-walk algorithm (Christen et al., 2010).

Table 1
Test and case scenarios to assess adequacy in testing for training periods.

Scenario	Sub-scenario	Classification
Testing and cases increase, $T_i \geq T_{i-1}, c_i \geq c_{i-1}$	Cases increase faster than testing, then $r_i^T \leq r_i^c$	Not adequate
	Testings increases faster than cases, then $r_i^T \geq r_i^c$	Adequate
Testing and cases decrease, $T_i < T_{i-1}$, $c_i < c_{i-1}$	Testing decreases faster than cases, then $r_i^T < r_i^c$	Not adequate
	Cases decrease faster than tests, then $r_i^T > r_i^c$	Adequate
Testing increases and cases decrease, $T_i \geq T_{i-1}, c_i < c_{i-1}$	Then, $r_i^T \geq r_i^c$	Adequate
Testing decrease and cases increase, $T_i < T_{i-1}, c_i \geq c_{i-1}$	Then, $r_i^T \leq r_i^c$	Not adequate

2.7.1.2. Duration of viral shedding. The deviance information criterion (DIC) was used to select the shedding time (m). DIC is a Bayesian generalization of the Akaike information criterion (AIC) for model selection in a finite set of models, with preference given to models with lower DIC. The DIC is preferred in settings with Bayesian model selection problems where the model's posterior distributions are obtained by MCMC simulation (Spiegelhalter et al., 2002). We selected the appropriate shedding time by computing DIC in a grid search along the parameter space $m : \{6, \ldots, 10\}$ (Benefield et al., 2020).

2.7.2. Simple linear regression model

Let $\tilde{\mathbf{I}} = (\tilde{I}_1, \tilde{I}_2, \ldots, \tilde{I}_n)$ be the vector of 7-day moving average of cases (smoothed cases) and $\mathbf{C} = (C_1, C_2, \ldots, C_n)$ be the vector of WW data. We assume the following noise model,

$$\log(\tilde{I}_i) = \beta \log(C_i) + \varepsilon_i, \quad i = 1, \ldots, n \tag{4}$$

where ε_i is a random residual associated with observation i which is assumed to be distributed as $N(0, \sigma^2)$, with σ^2 as the residual variance. This inference problem aims to estimate $\theta = (\beta, \sigma)$ from WW data and smoothed cases. A log-linear model is assumed to address positively skewed data and prevent negative fitted values.

2.8. Selection of model training periods

We describe whether or not testing is adequate in a particular period of observed cases by calculating the rate of change in tests conducted and new cases within a specific time period. We define the rate of change of both tests conducted (r_i^T) and confirmed positive cases (r_i^c) during period i as $r_i^T = T_i/T_{i-1}$ and $r_i^c = c_i/c_{i-1}$, respectively, where T_{i-1}, T_i denote the number of tests carried out in two consecutive periods, and c_{i-1}, c_i denote the number of positive cases detected in these periods. We classify a testing period as adequate when the rate of change in testing is greater than the rate of change in cases; otherwise, if the rate of change in testing is lower/equal to the rate of change in cases, we conclude that the testing period is inadequate. We summarize various scenarios of testing adequacy in Table 1. Our determination of testing adequacy, and thus suitability for model training for both linear and deconvolution models, assumes that observed cases would be sufficiently close to true cases when testing rates are high compared to case rates and test positivity remains low as determined through the community screening programs.

2.9. Effective reproductive number

The number of people in a population who are susceptible to infection by an infected individual at any particular time is denoted by R_e, the effective reproductive number. This dimensionless quantity is sensitive to time-dependent variation due to reductions in susceptible individuals, changes in population immunity, and other factors. R_e can be estimated by the ratio of the number of new infections (I_t) generated at time t, to the total infectious individuals at time t, given by $\Sigma_{s=1}^{t} I_{t-s} w_s$, the sum of infection incidence up to time step $t-1$, weighted by the infectivity function w_s. We implemented Cori et al.'s (2013) approach to estimate R_e directly from observed cases and from cases that were estimated from the WW data.

3. Results

3.1. Identification of adequate training periods

We computed the rate of change in the number of tests and cases by week for Davis between December 1, 2021, and March 31, 2022 (Fig. 2). Each week was compared with a previous week and classified as

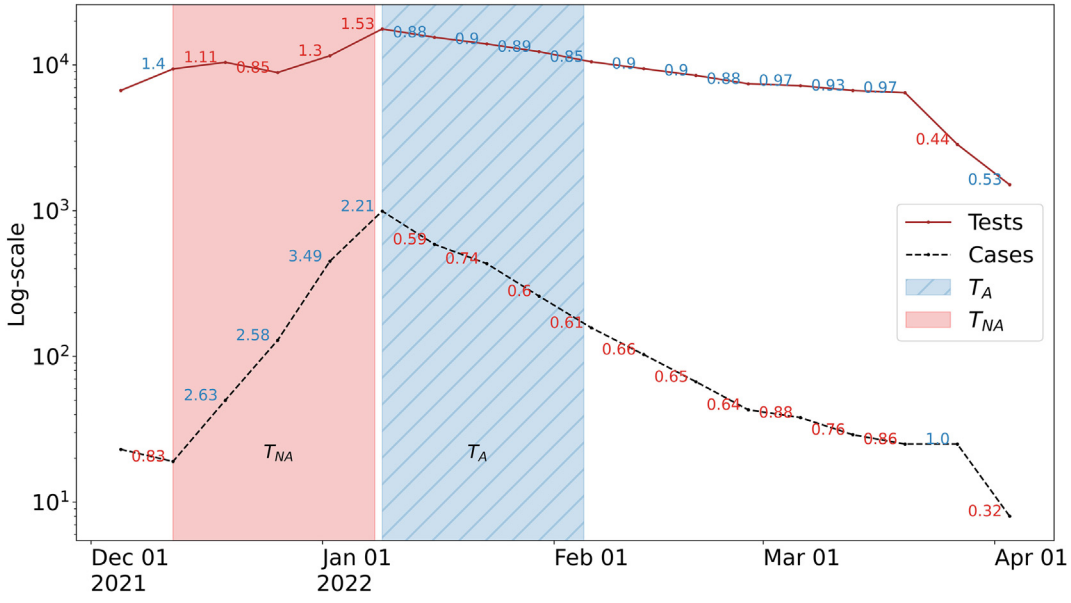

Fig. 2. On a log scale, the number of tests administered in Davis (solid line) and cases (dashed line) by week. The week-to-week rate of change in cases and tests are displayed; blue numbers indicate the test rate is greater than the case rate, and red numbers are the opposite. The blue and red shaded region corresponds training periods with Adequate (T_A) and Not Adequate (T_{NA}) testing.

adequate whenever the rate of change in tests was greater than the rate of change in cases and as not adequate otherwise.

Fig. 2 illustrates two specific training periods assumed for the analysis of Davis. The first training period includes data from December 12, 2021, to January 8, 2022 (denoted by T_{NA}), and the second training period assumes data from January 9 to February 2, 2022 (denoted by T_A). A training period designated by T_{NA} (Not Adequate) corresponds to a scenario where the test rate is consistently lower than the rate of new cases. Similarly, a training period denoted by T_A corresponds to a scenario where the testing rate exceeds the rate of new cases. We assess testing adequacy for Woodland and UC Davis (Figs. C.1 and D.1); similarly identified a period of inadequate testing prior to an observed surge in infections.

3.2. Comparison of models to estimate public health metrics from wastewater data

We applied a deconvolution technique and a linear regression to reconstruct incident cases of COVID-19 from the WW data, assuming model training periods according to the adequacy of clinical testing efforts. We found that the magnitude of case projections and trends was sensitive to the assumption of the model training period for both model constructs (Fig. 3). However, the timing of peaks in cases predicted was independent of the training period.

Case predictions from the models that assumed a training period with inadequate testing (T_{NA}) were consistently lower than projections from the models that assumed a training period with adequate testing (T_A), and also lower than observed cases mostly. These results and our assumption that true cases are above that of observed cases suggest that models using T_{NA} systematically underestimated true cases. This finding is consistent with our expectations since fewer cases are detected during T_{NA} than T_A periods. Projection of cases from models that assumed T_A aligned more consistently with observed cases in periods where testing was deemed adequate. The difference in case predictions from the two training periods was particularly evident in January 2021, during the onset of the Omicron variant surge in Davis.

Case projections from the linear model that assumed T_A were able to capture the peak of the observed cases more closely than the deconvolution model, although with greater uncertainty. It is worth noting that results from the deconvolution and the linear models are similar because the linear model is fitted with the 7-day moving-average of case data. Data smoothing of this kind corresponds to a convolution with equal daily weights. The estimation of cases from the linear model assuming T_{NA} was similar to the results of the deconvolution model, Fig. 3B.

R_e monitors changes in disease transmission over time, assesses the effectiveness of interventions, and can be useful in guiding policy decision-making. Estimates of R_e from the median of the predicted cases using the deconvolution and linear models are similar. In most of the period assessed, R_e determined from WW results are quite similar in magnitude and follow the trends for R_e calculated using observed cases (Fig. 4B). A notable difference between the R_e estimated with the observed cases and that obtained with the WW data, using both the linear and the deconvolution model, occurs in mid-March and days that followed. In mid-March, the median of R_e estimated with observed cases was above 1, and the medians of R_e estimated with WW data for the linear and deconvolution model were below 1. Later, the behavior was opposite; R_e for cases was below 1, and the medians of R_e with WW data for the linear and deconvolution model were above 1. During these periods, the observed cases (I_i) were between 0 and 8 per day, with many days of zeros. These low counts make the calculation of R_e with the observed cases unreliable. As recommended by Cori et al. (2013), R_e should only be estimated for incidence greater than 10, $I_i \geq 10$. On the other hand, the predictive median of the cases with which we calculate the R_e was between 7 and 11 cases per day, making the calculation of R_e more reliable than those computed based on observed cases. The posterior analysis using the estimated R_e from WW data thus indicates

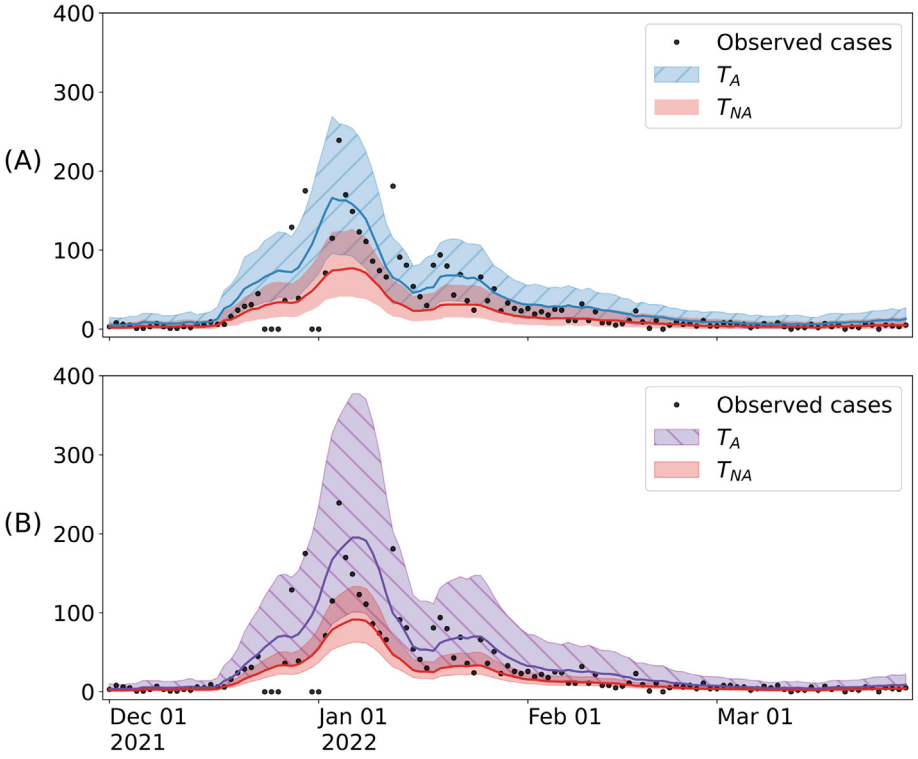

Fig. 3. Predicted cases assuming the deconvolution (A) and linear (B) models. Estimated cases using an adequate (T_A) training period for each model are displayed in blue/purple; results assuming an inadequate (T_{NA}) period are shown in red. Solid lines and shaded regions illustrate the median and 95 % prediction intervals, respectively.

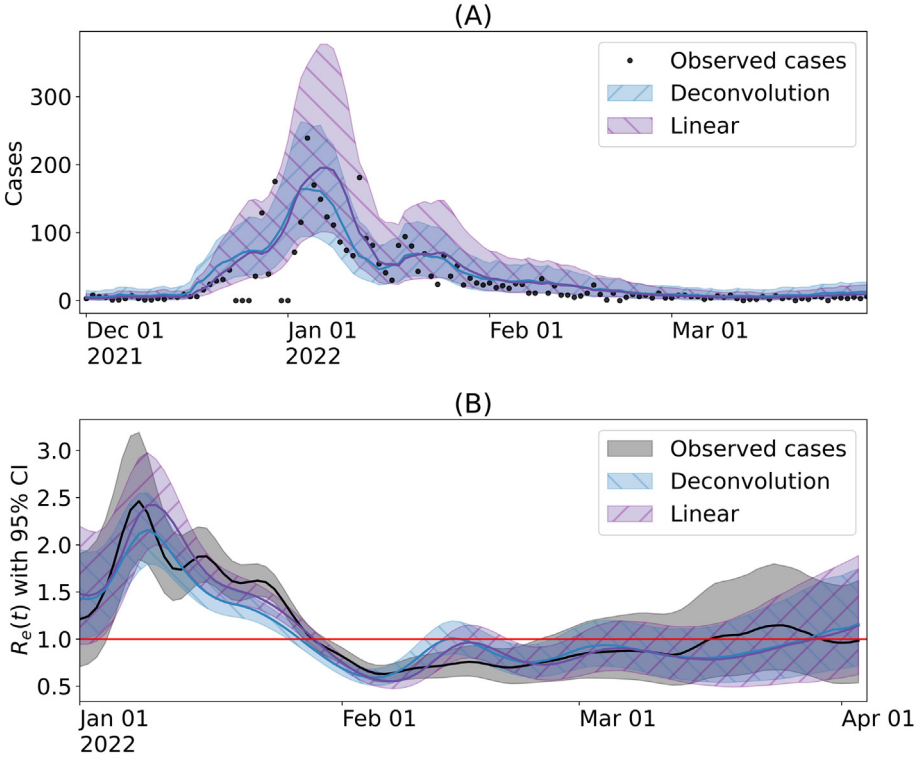

Fig. 4. (A) Predicted cases assuming the linear (purple) and the deconvolution models (blue), trained in the period classified as adequate. (B) Effective R_e of Davis computed with: observed cases (gray), the median of the cases estimated for the deconvolution model (blue) and the linear regression (purple).

that an outbreak ($R_e > 1$) may have occurred in Davis that was not detected through clinical cases (Fig. B.1).

While the magnitude of predicted cases differed with or without adequate training periods, similar trends in cases were obtained. This, in turn, was reflected in similar estimates of R_e (Fig. 5) since the estimate of R_e is scale-free. This finding shows that these models are able to track infection dynamics even with inadequate training periods.

We demonstrate the adaptability of our methodology using data for Woodland and UC Davis and present results in Appendices C and D, respectively. The trends of the observed cases are recovered with both models (Figs. C.2 and D.2), yielding results consistent with those obtained for Davis.

4. Discussion

Community-wide testing has played a critical role in mitigating the COVID-19 pandemic. However, large-scale testing has been limited and falls further behind during surges of infections. We developed criteria to classify the adequacy of clinical testing in a community through time, and we applied the classification scheme to three Northern California communities. As was observed in many other

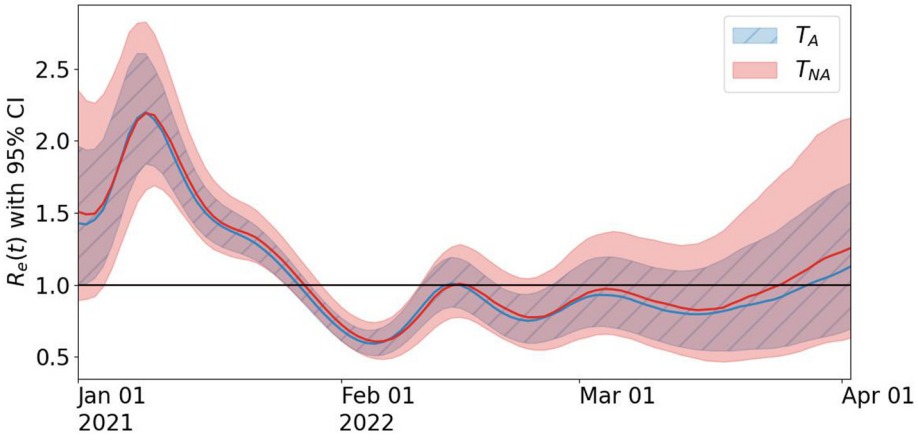

Fig. 5. R_e of Davis using the median of cases estimated assuming the deconvolution model with adequate (T_A) and inadequate (T_{NA}) training periods.

communities at the time, we found that clinical testing was inadequate at the front end of the wave of Omicron infections that occurred during our study period. Inadequate clinical testing during surges of infection makes it particularly challenging to discern true levels of SARS-CoV-2 infections in a population. WBE can fill data gaps caused by inadequate testing programs. As clinical testing transitions further towards at-home self-testing, measurements of SARS-CoV-2 RNA in WW can serve as an increasingly important indicator for COVID-19 transmission.

Myriad sources of variability and uncertainty in WW data can nevertheless impact the accuracy of estimates of COVID-19 cases or other public health metrics derived from WW data (Arabzadeh et al., 2021; Belia et al., 2009; Courbariaux et al., 2022; Li et al., 2021). Statistically representative samples can also be difficult to obtain because of the complexity of WW collection systems and the physical challenge of ensuring consistency in sample acquisition and processing (Panchal et al., 2021). Such challenges can limit the comparability of WW results across different WBE programs. The modeling framework we described to estimate COVID-19 cases from WW data accounts for uncertainty and relies on short training periods using clinical testing data to calibrate WW measurements to local conditions.

We showed that case projections reconstructed from either the Bayesian deconvolution or the simple linear model were generally higher than cases observed through clinical testing, particularly during periods with sub-optimal testing. These results are not surprising, as we expected that the WW models would yield case estimates higher than cases observed through screening, given that WW is not subject to the same selection biases as testing. While both the deconvolution and linear regression models captured the trends in observed cases overall, qualitative differences were evident between the approaches, particularly when testing was limited. Both models identified steep upward trends in cases during the surge in mid-January and at the onset of the Omicron surge Fig. 4A.

The classification approach we developed to assess the adequacy of model training periods was essential to providing robust estimates of case projections. Training periods that satisfied the proposed characteristics (i.e., adequate testing) resulted in similar estimates from each model and yielded trends consistent with observed cases. Case projections that assumed training periods with poor testing generally underestimated cases compared to projections from adequate training periods. While the proposed models do not seek to recover the curve of reported cases (an underestimate of actual cases, especially in a limited testing scenario), the use of adequate training periods for the WW models enabled us to capture trends in case counts much more closely. It is evident that training periods with inadequate testing introduce a downward bias into the model.

WBE has substantially lower resource requirements than mass diagnostic testing, and WW data lack bias from care- and test-seeking behavior in the catchment population. WBE programs that determine COVID-19 public health metrics at the community level can work as a powerful and cost-effective complement to other, more traditional intervention methods. The analytic methods presented here can inform local public health policy and community-level interventions, for instance, by helping to assess when the initiation of clinical screening programs and non-pharmaceutical interventions are needed. The model can be especially valuable to fill data gaps during surges of infection when clinical testing is inadequate and could be used to assess when estimates of case rates exceed certain thresholds. WBE does come with the inherent challenge of determining the populations being monitored, which is exacerbated if the population served is highly mobile (e.g., a university campus). In other words, WBE methods for tracking COVID-19 are inherently location-specific, whereas public screening programs are tied to the people they serve. The calibration of WW models using clinical data will be most robust in places with minimal mobility or within adequately described and understood populations.

With screening programs winding down across the United States, finding training periods with adequate testing rates may not be feasible. In such cases, applying the deconvolution model for WBE can still highlight important trends. A periodic sentinel system could be employed to produce sufficient prevalence estimates for training periods where tests are only administered for clinical diagnostics. Such a system would recruit a representative population sample for repeated testing during a training period to establish a baseline, enabling the WW deconvolution model to track incidence for an extended period of time. The same sentinel group could be called back later when the model needs to be updated to retrain for new situations.

WBE surveillance systems should be cognizant that they are not unduly targeting and stigmatizing vulnerable communities. WBE is much less invasive than diagnostic testing and protects individual identities, thereby avoiding the stigmatization of individuals and not requiring individual consent (Murakami et al., 2020). Yet focusing too heavily on public surveillance efforts can negatively influence public perception of those being monitored (Sims and Kasprzyk-Hordern, 2020). Mathematical models that employ machine learning, such as the deconvolution model described herein, must be trained with data sets that are not sampled by biased collection methods, else they may inadvertently reintroduce social biases into the results and contribute to larger inequities in public health.

Overall, both models presented can capture disease trends with few assumptions. At least two wastewater samples per week are needed to provide accurate estimates of trends (Huisman et al., 2022; Keshaviah et al., 2021). To ensure reliable estimates for case counts, we suggest a minimum of three consecutive weeks of training periods classified as adequate, or as close to this as possible.

This study has some limitations that are worth noting. The proposed models are validated based on observed cases and are limited by their dependence on adequate training periods. The latter limitation becomes more significant as testing efforts are scaled down or as historical data on adequate testing is lacking. However, even with limited testing, our model is able to track disease trends, providing reliable estimates of R_e. Our modeling framework may also lack accuracy in long-term predictions when the relationship between wastewater and cases changes over time, as it is observed with the emergence of new variants (Frampton et al., 2021; Graham et al., 2021). To address this limitation, adaptive models should be considered to allow for the re-calibration of parameters over time.

5. Significance

- We proposed a method to characterize training periods based on testing and clinical case rates.
- A training period is classified as adequate when the rate of change in tests exceeds the rates of change in cases.
- We proposed two models to relate wastewater to clinical cases: a linear model and a deconvolution model with a Bayesian approach.
- We show that case predictions from models that assumed inadequate (T_{NA}) training periods were consistently lower than projections from the models that assumed a training period with adequate testing (T_A).
- While the magnitude of predicted cases depended on training periods, similar case trends were observed. This, in turn, was reflected in similar estimates of R_e, suggesting that the models are able to track infection dynamics even with inadequate training periods.

Human participant protection

This study was determined to be exempt from institutional review board review by the UC Davis Office of Research.

CRediT authorship contribution statement

M.L.D.T and **J.C.M.L.**: Conceptualization, Methodology, Software, Formal analysis, Writing - Original draft preparation, Writing -

Reviewing & Editing. **M.K.**: analytical assay development and quality control, writing methods. **R.O.**: laboratory process management, quality control, data collection, writing methods. **L.R.** and **C.W.B.**: laboratory processing and wastewater data collection, writing methods. **L.T.**: literature review and initial model evaluation. **L.T.** and **M.S.**: partner engagement and project management. **Y.E.G.** and **A.J.S.**: literature review, Writing - Reviewing & Editing. **K.S.** and **C.N.**: wastewater monitoring project supervision. **B.H.P.**: Healthy Davis Together project PI, Writing - Reviewing & Editing. **M.N.**: Methodology, research oversight/supervision, Writing - Reviewing & Editing. **H.N.B.**: Healthy Central Valley Together project PI; project conception, funding, research oversight and collaborator coordination, Writing - Reviewing & Editing.

Data availability

The codes implemented for the study are available in the GitHub repository (Daza-Torres and Montesinos-López, 2022). Analyses were carried out using Python version 3.

Declaration of competing interest

The authors declare that they have no known competing financial interests or personal relationships that could have appeared to influence the work reported in this paper.

Acknowledgments

This research was supported by the Healthy Central Valley Together (HCVT) and Healthy Davis Together (HDT) programs at the University of California, Davis. This research was also partly supported by the NIH Rapid Acceleration of Diagnostics (RADxSM) initiative with federal funds from the National Institute of Biomedical Imaging and Bioengineering, National Institutes of Health. The current contract is funded by the Public Health and Social Services Emergency Fund through the Biomedical Advanced Research and Development Authority, HHS Office of the Assistant Secretary for Preparedness and Response, Department of Health and Human Services, under Contract No. 75N92021C00012. All authors reviewed and approved the final manuscript.

Appendix A. Additional information on the ddPCR assay designs

Table A.1
RT-ddPCR primers and probes used in this study.

Target	Primer/probe sequence (5′, 3′)		Amplicon length	Source/reference
SARS-CoV-2; N1 gene	Forward	GACCCCAAAATCAGCGAAAT	72	U.S. Centers for Disease Control and Prevention (CDC) (CDC, 2022)
	Reverse	TCTGGTTACTGCCAGTTGAATCTG		
	Probe	ACCCCGCATTACGTTTGGTGGACC (5′FAM/ZEN/3′Iowa Black FQ)		
SARS-CoV-2; N2 gene	Forward	TTACAAACATTGGCCGCAAA	67	
	Reverse	GCGCGACATTCCGAAGAA		
	Probe	ACAATTTGCCCCCAGCGCTTCAG (5′SUN/ZEN/3′Iowa Black FQ)		
BCoV; transmembrane gene	Forward	CTGGAAGTTGGTGGAGTT	85	Decaro et al. (2008)
	Reverse	ATTATCGGCCTAACATACATC		
	Probe	CCTTCATATCTATACACATCAAGTTGTT (5′HEX/ZEN/3′Iowa Black FQ)		
PMMoV; coat protein gene	Forward	GAGTGGTTTGACCTTAACGTTTGA	68	Haramoto et al. (2013) and This study (for probe modification)
	Reverse	TTGTCGGTTGCAATGCAAGT		
	Probe	CCTA + C + C + GAAGCA + A + A + TG[a] (5′FAM/3′Iowa Black FQ)		

[a] The Affinity Plus™ probe (IDT) with locked nucleic acids (marked as +) was used to increase the hybridization melt temperature of shorter sequences of the PMMoV probe.

Table A.2
Preparation of the duplex One-Step RT-ddPCR reaction.

Component	Volume per reaction, μL	Final concentration
Supermix (4×)	5.5	1×
Reverse transcriptase	2.2	20 U/μL
30 mM DTT	1.1	15 mM
20X P/P Mix (Ch 1 dye: FAM)	1.1	1×
20X P/P Mix (Ch2 dye: Sun (a.k.aVIC) or HEX)	1.1	1×
Nuclease-free water	5.5	–
Subtotal (Mastermix)	16.5	–
RNA sample	5.5	–
Total volume (Mastermix + sample) (volume include 10 % excess in setup)	22.0	–

Table A.3
Preparation of 20× primer/probe Mix (p/p Mix).

Target	Recipe			
	Reagent	Initial concentration	Volume added (μL)	Final concentration in ddPCR reaction
20× p/p Mix	Forward	100 μM	45.0	900 nM
	Reverse	100 μM	45.0	900 nM
	Probe	100 μM	12.5	250 nM
	Nuclease-free water	–	147.5	–
	Total volume		250	

Table A.4
Synthesized gene fragments used for positive controls in ddPCR.

Target	Sequences (5′ - 3′)	Reference gene GenBank ID	Ordered from
N1	GACGTTCGTGTTGTTTTAGATTTCATCTA AACGAACAAACTAAAATGTCTGATAATGG ACCCCAAAA TCAGCGAAATGCACCCCGCA TTACGTTTGGTGGACCCTCAGATTCAACT GGCAGTAACCAGAATGGAG AACGCAGTGG GGCGCGATCAAAACAACGTCGGCCCCAAG GTTTACCCAATAATACTGCGTCTTGG	MN975262	Eurofins
N2	ACGTGGTCCAGAACAAACCCAAGGAAATTT TGGGGACCAGGAACTAATCAGACAAGGAAC TGATTA CAAACATTGGCCGCAAATTGCACA ATTTGCCCCCAGCGCTTCAGCGTTCTTCGG AATGTCGCGCATTG GCATGGAAGTCACACC TTCGGGAACGTGGTTGACCTACACAGGTGC CATCAAATTGGATGACAAAG	MN975262	Eurofins
PMMoV	TTTTCCCGGATGTGTAATACATTAGGCGTA GATCCATTGGTGGCAGCAAAGGTAATGGTA GCTGTGGTT TCAAATGAGAGTGGTTTGACC TTAACGTTTGAGAGGCCTACCGAAGCAAAT GTCGCACTTGCATTGCAAC CGACAATTACA TCAAAGGAGGAAGGTTCGTTGAAGATTGTG TCGTCAGACGTAGGTGAGTC	M81413	IDT
BCoV	GCCATTATCATGTGGATTGTGTATTTTGTG AATAGTATCAGGTTGTTTATTAGAACTGGA AGTTGGTGG AGTTTCAACCCAGAAACAAAC AACTTGATGTGTATAGATATGAAGGGAAGG ATGTATGTTAGGCCGAT AATTGAGGACTAC CATACCCTTACGGTCACAATAATACGTGGT CATCTTTACATGCAAGGTAT	U00735	IDT

Table A.5
Limit of blank and limit of detection.

	LoB (rank)	STD	Theoretical LOD
Conc (copies/mL of wastewater)			
N1	13.605	5.547	24.700
N2	18.544	6.712	31.967
Conc (copies/20 μL reaction)			
N1	3.401	1.387	6.175
N2	4.636	1.678	7.992

Appendix B. Additional results for Davis

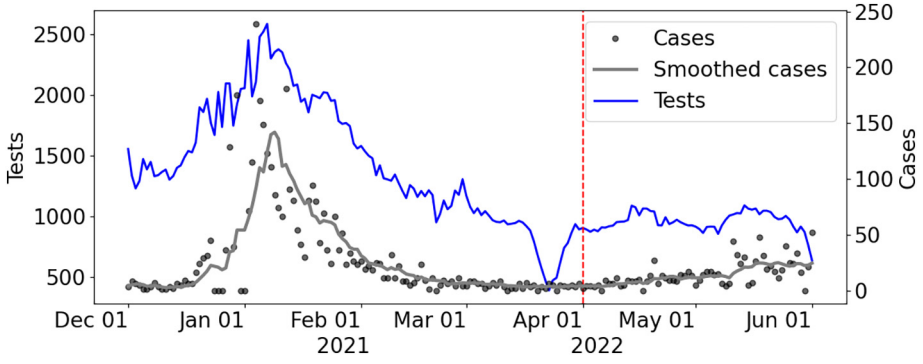

Fig. B.1. Davis. Raw cases (Cases), 7-day moving average of cases (Smoothed cases), and number of tests administered (Tests).

Appendix C. Results for City of Woodland

Fig. C.1A illustrates data from Woodland that was used to reconstruct cases from WW. Fig. C.1B described the 7-day moving average for cases (Smoothed cases) and 10-day trimmed average for WW data (Smoothed N/PMMov). Fig. C.1C illustrates the two specific training periods assumed for the analysis. The first training period includes data from December 11 to December 30, 2021 (denoted by T_{NA}), and the second training period assumes data from January 13 to February 2, 2022 (denoted by T_A).

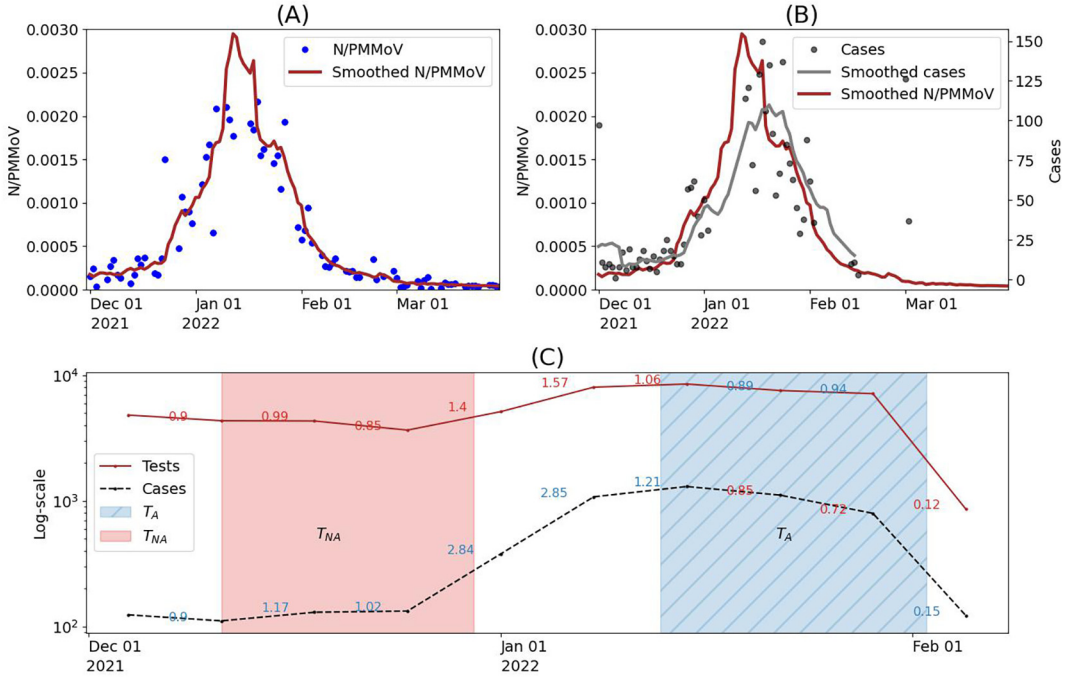

Fig. C.1. City of Woodland. (A) Raw wastewater data (N/PMMoV) and 10-day trimmed average of WW data (Smoothed N/PMMoV). (B) Raw cases (Cases), 7-day moving average of cases (Smoothed cases), and 10-day trimmed average of WW data. (C) On a log scale, the number of tests administered (solid line) and cases (dashed line) by week. The week-to-week rate of change in cases and tests are displayed; blue numbers indicate the test rate is greater than the case rate, and red numbers are the opposite. The blue and red shaded region corresponds training periods with Adequate (T_A) and Not Adequate (T_{NA}) testing.

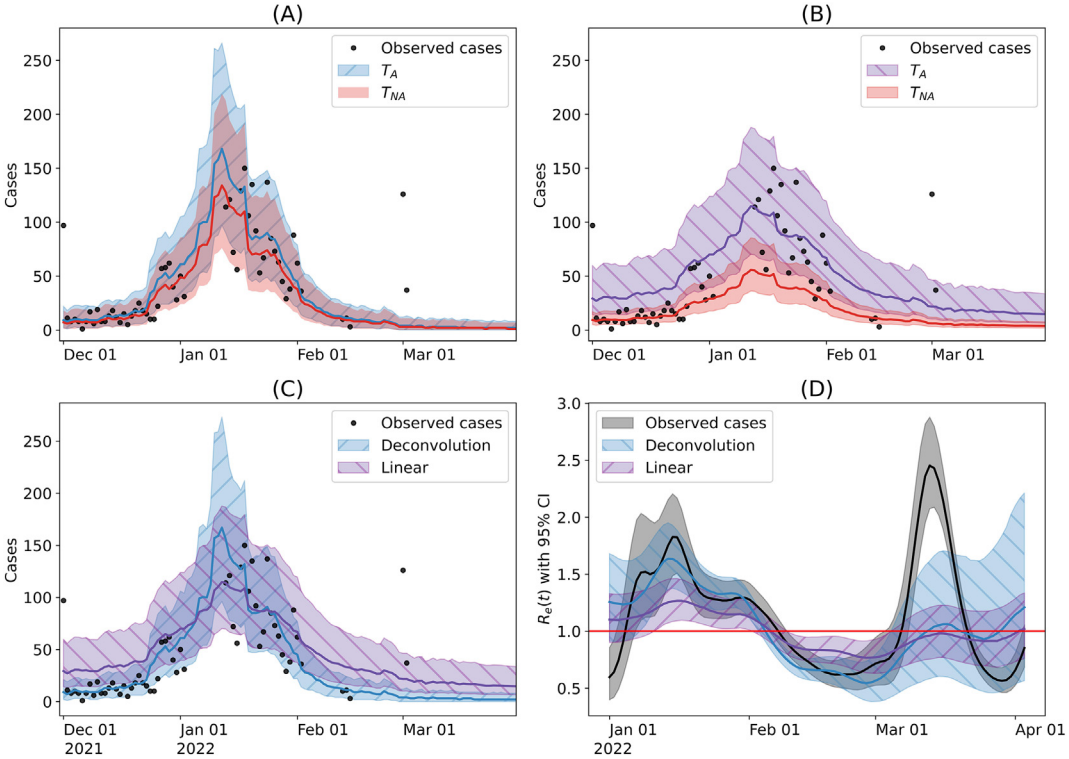

Fig. C.2. City of Woodland. Predicted cases assuming the deconvolution (A) and linear (B) models. Estimated cases using an adequate (T_A) training period for each model are displayed in blue/purple; results assuming an inadequate (T_{NA}) period are shown in red. Solid lines and shaded regions illustrate the median and 95 % prediction intervals, respectively. (C) Predicted cases assuming the linear (purple) and the deconvolution models (blue), trained in the period classified as adequate. (D) Effective R_e computed with: observed cases (gray), the median of the cases estimated for the deconvolution model (blue), and the linear regression (purple).

Appendix D. Results for UC Davis

Fig. D.1A illustrates data from Woodland that was used to reconstruct cases from WW. Fig. D.1B described the 7-day moving average for cases (Smoothed cases) and the 10-day trimmed average for WW data (Smoothed N/PMMov). Fig. D.1C illustrates the two specific training periods assumed for the analysis. The first training period includes data from December 12, 2021, to January 3, 2022 (shaded in red, denoted by T_{NA}), and the second training period assumes data from January 12 to February 3, 2022 (shaded in blue, denoted by T_A).

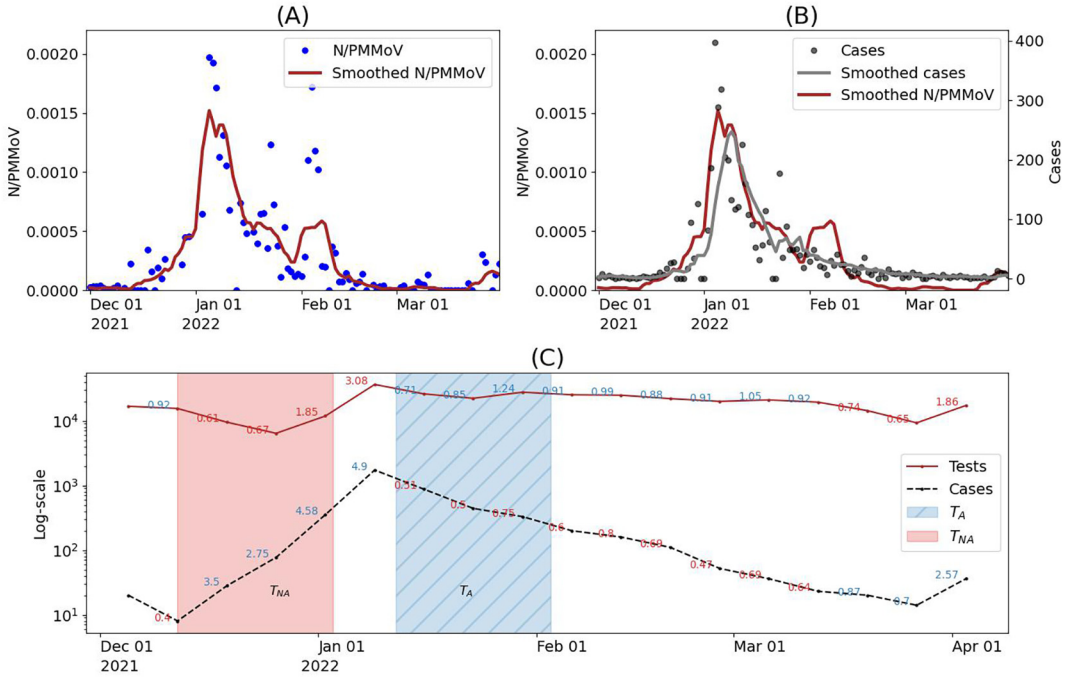

Fig. D.1. UC Davis. (A) Raw wastewater data (N/PMMoV) and 10-day trimmed average of WW data (Smoothed N/PMMoV). (B) Raw cases (Cases), 7-day moving average of cases (Smoothed cases), and 10-day trimmed average of WW data. (C) On a log scale, the number of tests administered (solid line) and cases (dashed line) by week. The week-to-week rate of change in cases and tests are displayed; blue numbers indicate the test rate is greater than the case rate, and red numbers are the opposite. The blue and red shaded region corresponds training periods with Adequate (T_A) and Not Adequate (T_{NA}) testing.

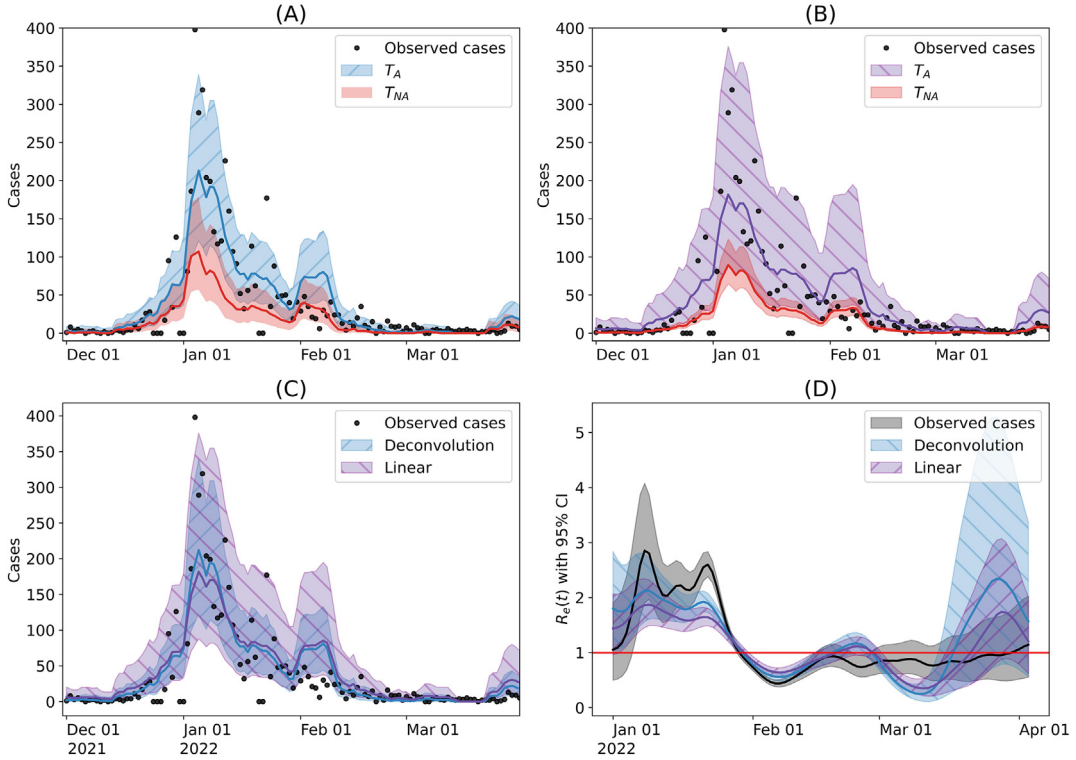

Fig. D.2. UC Davis. Predicted cases assuming the deconvolution (A) and linear (B) models. Estimated cases using an adequate (T_A) training period for each model are displayed in blue/purple; results assuming an inadequate (T_{NA}) period are shown in red. Solid lines and shaded regions illustrate the median and 95 % prediction intervals, respectively. (C) Predicted cases assuming the linear (purple) and the deconvolution models (blue), trained in the period classified as adequate. (D) Effective R_e computed with: observed cases (gray), the median of the cases estimated for the deconvolution model (blue), and the linear regression (purple).

References

Ahmed, W., Bivins, A., Bertsch, P.M., Bibby, K., Choi, P.M., Farkas, K., Gyawali, P., Hamilton, K.A., Haramoto, E., Kitajima, M., et al., 2020. Surveillance of sars-cov-2 rna in wastewater: methods optimization and quality control are crucial for generating reliable public health information. Curr. Opin. Environ. Sci. Health 17, 82–93. https://doi.org/10.1016/j.coesh.2020.09.003.

Arabzadeh, R., Grünbacher, D.M., Insam, H., Kreuzinger, N., Markt, R., Rauch, W., 2021. Data filtering methods for sars-cov-2 wastewater surveillance. Water Sci. Technol. 84 6(0), 1324–1339. https://doi.org/10.2166/wst.2021.343.

Asghar, H., Diop, O.M., Weldegebriel, G., Malik, F., Shetty, S., El Bassioni, L., Akande, A.O., Al Maamoun, E., Zaidi, S., Adeniji, A.J., et al., 2014. Environmental surveillance for polioviruses in the global polio eradication initiative. J. Infect. Dis. 210 (suppl_1), S294–S303. https://doi.org/10.1093/infdis/jiu384.

Belia, E., Amerlinck, Y., Benedetti, L., Johnson, B., Sin, G., Vanrolleghem, P.A., Gernaey, K., Gillot, S., Neumann, M., Rieger, L., et al., 2009. Wastewater treatment modelling: dealing with uncertainties. Water Sci. Technol. 60 (8), 1929–1941. https://doi.org/10.2166/wst.2009.225.

Benefield, A.E., Skrip, L.A., Clement, A., Althouse, R.A., Chang, S., Althouse, B.M., 2020. Sars-cov-2 viral load peaks prior to symptom onset: a systematic review and individual-pooled analysis of coronavirus viral load from 66 studies. medRxiv. https://doi.org/10.1101/2020.09.28.20202028.

Biorad, 2021. A practical guide for evaluating detection capability using ddPCR. https://www.bio-rad.com/en-us/life-science/learning-center/introduction-to-digital-pcr. (Accessed 23 May 2022).

Castiglioni, S., Thomas, K.V., Kasprzyk-Hordern, B., Vandam, L., Griffiths, P., 2014. Testing wastewater to detect illicit drugs: state of the art, potential and research needs. Sci. Total Environ. 487, 613–620. https://doi.org/10.1016/j.scitotenv.2013.10.034.

CDC, 2022. 2019-Novel Coronavirus (2019-nCoV) Real-Time RT-PCR Diagnostic Panel. https://www.fda.gov/media/134922/download.

Cevik, M., Tate, M., Lloyd, O., Maraolo, A.E., Schafers, J., Ho, A., 2020. Sars-cov-2, sars-cov-1 and mers-cov viral load dynamics, duration of viral shedding and infectiousness: a living systematic review and meta-analysis. SARS-CoV-1 and MERS-CoV viral load dynamics, duration of viral hedding and infectiousness. A Living Systematic Review and Meta-Analysis. https://doi.org/10.2139/ssrn.3677918.

Choi, P.M., Tscharke, B., Samanipour, S., Hall, W.D., Gartner, C.E., Mueller, J.F., Thomas, K.V., O'Brien, J.W., 2019. Social, demographic, and economic correlates of food and chemical consumption measured by wastewater-based epidemiology. Proc. Natl. Acad. Sci. 116 (43), 21864–21873. https://doi.org/10.1073/pnas.1910242116.

Christen, J.A., Fox, C., et al., 2010. A general purpose sampling algorithm for continuous distributions (the t-walk). Bayesian Anal. 5 (2), 263–281. https://doi.org/10.1214/10-BA603.

Cori, A., Ferguson, N.M., Fraser, C., Cauchemez, S., 2013. A new framework and software to estimate time-varying reproduction numbers during epidemics. Am. J. Epidemiol. 178 (9), 1505–1512. https://doi.org/10.1093/aje/kwt133.

Courbariaux, M., Cluzel, N., Wang, S., Maréchal, V., Moulin, L., Wurtzer, S., Mouchel, J.-M., Maday, Y., Obépine consortium, J.-M., Nuel, G., 2022. A flexible smoother adapted to censored data with outliers and its application to sars-cov-2 monitoring in wastewater. arXiv. https://arxiv.org/abs/2108.02115v3.

COVIDPoops19, 2021. Summary of global sars-cov-2 wastewater monitoring efforts by uc merced researchers. https://www.arcgis.com/apps/dashboards/c778145ea5bb4daeb58d31afee389082 (Accessed on 06/14/2022).

Daza-Torres, M.L., Montesinos-López, J.C., 2022. Model training periods impact estimation of covid-19 incidence from wastewater viral loads. https://github.com/mdazatorres/WWdeconvolution_model.

Decaro, N., Elia, G., Campolo, M., Desario, C., Mari, V., Radogna, A., Colaianni, M.L., Cirone, F., Tempesta, M., Buonavoglia, C., 2008. Detection of bovine coronavirus using a taqman-based real-time rt-pcr assay. J. Virol. Methods (ISSN: 0166-0934) 151 (2), 167–171. https://doi.org/10.1016/j.jviromet.2008.05.016. https://www.sciencedirect.com/science/article/pii/S016609340800181X.

Frampton, D., Rampling, T., Cross, A., Bailey, H., Heaney, J., Byott, M., Scott, R., Sconza, R., Price, J., Margaritis, M., et al., 2021. Genomic characteristics and clinical effect of the emergent sars-cov-2 b.1.1.7 lineage in london, uk: a whole-genome sequencing and hospital-based cohort study. Lancet Infect. Dis. (ISSN: 1473-3099) 21 (9), 1246–1256. https://doi.org/10.1016/S1473-3099(21)00170-5.

Galani, A., Aalizadeh, R., Kostakis, M., Markou, A., Alygizakis, N., Lytras, T., Adamopoulos, P.G., Peccia, J., Thompson, D.C., Kontou, A., et al., 2022. Sars-cov-2 wastewater surveillance data can predict hospitalizations and icu admissions. Sci. Total Environ. 804, 150151. https://doi.org/10.1016/j.scitotenv.2021.150151.

Goldstein, E., Dushoff, J., Ma, J., Plotkin, J.B., Earn, D.J., Lipsitch, M., 2009. Reconstructing influenza incidence by deconvolution of daily mortality time series. Proc. Natl. Acad. Sci. 106 (51), 21825–21829. https://doi.org/10.1073/pnas.0902958106.

Graham, M.S., Sudre, C.H., May, A., Antonelli, M., Murray, B., Varsavsky, T., Kläser, K., Canas, L.S., Molteni, E., Modat, M., et al., 2021. Changes in symptomatology, reinfection, and transmissibility associated with the sars-cov-2 variant b. 1.1. 7: an ecological study. Lancet Public Health (ISSN: 2468-2667) 6 (5), e335–e345. https://doi.org/10.1016/S2468-2667(21)00055-4.

Haramoto, E., Kitajima, M., Kishida, N., Konno, Y., Katayama, H., Asami, M., Akiba, M., 2013. Occurrence of pepper mild mottle virus in drinking water sources in Japan. Appl. Environ. Microbiol. 79 (23), 7413–7418. https://doi.org/10.1128/AEM.02354-13.. https://journals.asm.org/doi/abs/10.1128/AEM.02354-13.

HDT, 2020. Healthy Davis Together. https://healthydavistogether.org/testing-data/. (Accessed 23 May 2022).

Hill, K., Zamyadi, A., Deere, D., Vanrolleghem, P.A., Crosbie, N.D., 2020. SARS-CoV-2 known and unknowns, implications for the water sector and wastewater-based epidemiology to support national responses worldwide: early review of global experiences with the COVID-19 pandemic. Water Qual. Res. J. (ISSN: 1201-3080) 56 (2), 57–67. https://doi.org/10.2166/wqrj.2020.100.

Huisman, J.S., Scire, J., Caduff, L., Fernandez-Cassi, X., Ganesanandamoorthy, P., Kull, A., Scheidegger, A., Stachler, E., Boehm, A.B., Hughes, B., et al., 2022. Wastewater-based estimation of the effective reproductive number of sars-cov-2. Environ. Health Perspect. 130 (5), 057011. https://doi.org/10.1289/EHP10050.

HYT, 2021. Healthy Yolo Together. https://healthydavistogether.org/. (Accessed 23 May 2022).

Karthikeyan, S., Ronquillo, N., Belda-Ferre, P., Alvarado, D., Javidi, T., Longhurst, C.A., Knight, R., Cristea, I.M., 2021. High-throughput wastewater sars-cov-2 detection enables forecasting of community infection dynamics in San Diego county. mSystems 6(2): e00045–21. https://doi.org/10.1128/mSystems.00045-21.

Keshaviah, A., Hu, X.C., Henry, M., 2021. Developing a flexible national wastewater surveillance system for covid-19 and beyond. Environ. Health Perspect. 129 (4), 045002. https://doi.org/10.1289/EHP8572. https://ehp.niehs.nih.gov/doi/abs/10.1289/EHP8572.

Kirby, A.E., Welsh, R.M., Marsh, Z.A., Yu, A.T., Vugia, D.J., Boehm, A.B., Wolfe, M.K., White, B.J., Matzinger, S.R., Wheeler, A., et al., 2022. Notes from the field: early evidence of the sars-cov-2 b. 1.1. 529 (omicron) variant in community wastewater—United States, November–December 2021. Morb. Mortal. Weekly Rep. 71 (3), 103–105. https://doi.org/10.15585/mmwr.mm7103a5.

Li, X., Zhang, S., Shi, J., Luby, S.P., Jiang, G., 2021. Uncertainties in estimating sars-cov-2 prevalence by wastewater-based epidemiology. Chem. Eng. J. 415, 129039. https://doi.org/10.1016/j.cej.2021.129039.

Lindén, A., Mäntyniemi, S., 2011. Using the negative binomial distribution to model overdispersion in ecological count data. Ecology 92 (7), 1414–1421. https://doi.org/10.1890/10-1831.1.

Mallapaty, S., et al., 2020. How sewage could reveal true scale of coronavirus outbreak. Nature 580 (7802), 176–177. https://doi.org/10.1038/d41586-020-00973-x.

Mardian, Y., Kosasih, H., Karyana, M., Neal, A., Lau, C.-Y., 2021. Review of current covid-19 diagnostics and opportunities for further development. Front. Med. 8. https://doi.org/10.3389/fmed.2021.615099 ISSN 2296–858X.

McMahan, C.S., Self, S., Rennert, L., Kalbaugh, C., Kriebel, D., Graves, D., Colby, C., Deaver, J.A., Popat, S.C., Karanfil, T., Freedman, D.L., 2021. Covid-19 wastewater epidemiology: a model to estimate infected populations. Lancet Planet. Health (ISSN: 2542-5196) 5 (12), e874–e881. https://doi.org/10.1016/S2542-5196(21)00230-8.

Medema, G., Been, F., Heijnen, L., Petterson, S., 2020a. Implementation of environmental surveillance for sars-cov-2 virus to support public health decisions: opportunities and challenges. Curr. Opin. Environ. Sci. Health 17, 49–71. https://doi.org/10.1016/j.coesh.2020.09.006.

Medema, G., Heijnen, L., Elsinga, G., Italiaander, R., Brouwer, A., 2020b. Presence of sars-coronavirus-2 rna in sewage and correlation with reported covid-19 prevalence in the early stage of the epidemic in the Netherlands. Environ. Sci. Technol. Lett. 7 (7), 511–516. https://doi.org/10.1021/acs.estlett.0c00357.

Mercer, T.R., Salit, M., 2021. Testing at scale during the covid-19 pandemic. Nat. Rev. Genet. 22, 415–426. https://doi.org/10.1038/s41576-021-00360-w.

Monteiro, S., Rente, D., Cunha, M.V., Gomes, M.C., Marques, T.A., Lourenço, A.B., Cardoso, E., Álvaro, P., Silva, M., Coelho, N., Vilaça, J., Meireles, F., Brôco, N., Carvalho, M., Santos, R., 2022. A wastewater-based epidemiology tool for covid-19 surveillance in portugal. (ISSN: 0048-9697) Sci. Total Environ. 804, 150264. https://doi.org/10.1016/j.scitotenv.2021.150264.

Murakami, M., Hata, A., Honda, R., Watanabe, T., 2020. Letter to the editor: wastewater-based epidemiology can overcome representativeness and stigma issues related to covid-19. Environ. Sci. Technol. 54 (9), 5311. https://doi.org/10.1021/acs.est.0c02172 PMID: 32323978.

Panchal, D., Prakash, O., Bobde, P., Pal, S., 2021. Sars-cov-2: sewage surveillance as an early warning system and challenges in developing countries. Environ. Sci. Pollut. Res. 28 (18), 22221–22240. https://doi.org/10.1007/s11356-021-13170-8.

Peccia, J., Zulli, A., Brackney, D.E., Grubaugh, N.D., Kaplan, E.H., Casanovas-Massana, A., Ko, A.I., Malik, A.A., Wang, D., Wang, M., et al., 2020. Measurement of sars-cov-2 rna in wastewater tracks community infection dynamics. Nat. Biotechnol. 38 (10), 1164–1167. https://doi.org/10.1038/s41587-020-0684-z.

Pillay, L., Amoah, I.D., Deepnarain, N., Pillay, K., Awolusi, O.O., Kumari, S., Bux, F., 2021. Monitoring changes in covid-19 infection using wastewater-based epidemiology: a South African perspective. Sci. Total Environ. (ISSN: 0048-9697) 786, 147273. https://doi.org/10.1016/j.scitotenv.2021.147273.

Raffle, A.E., Pollock, A.M., Harding-Edgar, L., 2020. Covid-19 mass testing programmes. BMJ 370. https://doi.org/10.1136/bmj.m3262.

Schoen, M.E., Wolfe, M.K., Li, L., Duong, D., White, B.J., Hughes, B., Boehm, A.B., 2022. Sars-cov-2 rna wastewater settled solids surveillance frequency and impact on predicted covid-19 incidence using a distributed lag model. ACS ES&T Water. https://doi.org/10.1021/acsestwater.2c00074.

Shah, S., Gwee, S.X.W., Ng, J.Q.X., Lau, N., Koh, J., Pang, J., 2022. Wastewater surveillance to infer covid-19 transmission: a systematic review. Sci. Total Environ. 804, 150060. https://doi.org/10.1016/j.scitotenv.2021.150060.

Sims, N., Kasprzyk-Hordern, B., 2020. Future perspectives of wastewater-based epidemiology: monitoring infectious disease spread and resistance to the community level. Environ. Int. 139, 105689. https://doi.org/10.1016/j.envint.2020.105689.

Spiegelhalter, D.J., Best, N.G., Carlin, B.P., Van Der Linde, A., 2002. Bayesian measures of model complexity and fit. J. R. Stat. Soc. Ser. B (Stat Methodol.) 64 (4), 583–639. https://doi.org/10.1111/1467-9868.00353.

Vallejo, J.A., Trigo-Tasende, N., Rumbo-Feal, S., Conde-Pérez, K., López-Oriona, Ángel, Barbeito, I., Vaamonde, M., Tarrío-Saavedra, J., Reif, R., Ladra, S., Rodiño-Janeiro, B.K., Nasser-Ali, M., Cid, Ángeles, Veiga, M., Acevedo, A., Lamora, C., Bou, G., Cao, R., Poza, M., 2022. Modeling the number of people infected with sars-cov-2 from wastewater

viral load in northwest Spain. Sci. Total Environ. (ISSN: 0048-9697) 811, 152334. https://doi.org/10.1016/j.scitotenv.2021.152334.

Vandenberg, O., Martiny, D., Rochas, O., van Belkum, A., Kozlakidis, Z., 2021. Considerations for diagnostic covid-19 tests. Nat. Rev. Microbiol. 19 (3), 171–183. https://doi.org/10.1038/s41579-020-00461-z.

Weiss, A., Jellingsø, M., Sommer, M.O.A., 2020. Spatial and temporal dynamics of sars-cov-2 in covid-19 patients: a systematic review and meta-analysis. EBioMedicine 58, 102916. https://doi.org/10.1016/j.ebiom.2020.102916.

Wolfe, M.K., Topol, A., Knudson, A., Simpson, A., White, B., Vugia, D.J., Yu, A.T., Li, L., Balliet, M., Stoddard, P., Han, G.S., Wigginton, K.R., Boehm, A.B., Langelier, C.R., 2021. High-frequency, high-throughput quantification of sars-cov-2 rna in wastewater settled solids at eight publicly owned treatment works in northern California shows strong association with covid-19 incidence. mSystems 6(5):e00829–21. https://doi.org/10.1128/mSystems.00829-21.

Wurtzer, S., Marechal, V., Mouchel, J., Maday, Y., Teyssou, R., Richard, E., Almayrac, J., Moulin, L., 2020. Evaluation of lockdown impact on sars-cov-2 dynamics through viral genome quantification in Paris wastewaters. medRxiv. https://doi.org/10.1101/2020.04.12.20062679.

Xu, C.L., Raval, M., Schnall, J.A., Kwong, J.C., Holmes, N.E., 2020. Duration of respiratory and gastrointestinal viral shedding in children with sars-cov-2: a systematic review and synthesis of data. Pediatr. Infect. Dis. J. 39 (9), e249–e256. https://doi.org/10.1097/INF.0000000000002814.

Zhu, Y., Oishi, W., Maruo, C., Saito, M., Chen, R., Kitajima, M., Sano, D., 2021. Early warning of covid-19 via wastewater-based epidemiology: potential and bottlenecks. Sci. Total Environ. (ISSN: 0048-9697) 767, 145124. https://doi.org/10.1016/j.scitotenv.2021.145124.

Zuccato, E., Chiabrando, C., Castiglioni, S., Calamari, D., Bagnati, R., Schiarea, S., Fanelli, R., 2005. Cocaine in surface waters: a new evidence-based tool to monitor community drug abuse. Environ. Health 4 (1), 1–7. https://doi.org/10.1186/1476-069X-4-14.